21st Australasian Fluid Mechanics Conference
Adelaide, Australia
10-13 December 2018

Curvature Effect on the Critical Rayleigh Number for the Instability of Natural Convection Boundary Layers

Y. Zhao, C. Lei and J.C. Patterson

Centre for Wind, Waves and Water
School of Civil Engineering, The University of Sydney, NSW 2006, Australia

Abstract

In the present study, curvature effects on the critical Rayleigh number Ra_c for the instability of natural convection boundary layers of Pr=7 on various isothermally heated vertical cylinders are investigated by direct stability analyses (DSA) with an axisymmetric numerical model. To determine the Ra_c, random temperature perturbations are introduced into a small region (2% of the total height) of the upstream heated surface near its leading edge. The slender cylinders under consideration span the aspect ratio $A=H/R_0$=2400, 960, 480 and 240, where H is the height of the cylinders and R_0 is the radius. A linear dependence of the critical Rayleigh number Ra_c on the aspect ratio A is obtained for the first time. The analyses of the kinetic energy balance further reveal that as the aspect ratio A increases, the boundary layer tends to be more stable since the ratio of energy production to dissipation reduces.

Introduction

One of the most important characteristics of a natural convection boundary layer instability is the critical Rayleigh number Ra_c (also characterized by critical Grashof number Gr in some literature) at which the flow becomes unstable. The boundary layers developing from an isothermally heated flat surface were studied theoretically and experimentally by Szewczyk [1], in which the Ra_c was determined to be 1.27×10^6 at Pr=10. In the context of differentially heated cavity flows, Ra_c was determined to be 6.8×10^5 by a direct stability analysis for the cavity at Pr=7.5 [2]. The Ra_c of the boundary layers over uniform flux vertical surfaces were also examined experimentally by Polymeropoulos *et al*. [3] and others.

While the instabilities of natural convection boundary layers on heated flat surfaces have been studied extensively [4-6], the instabilities of natural convection boundary layers adjacent to isothermally heated vertical slender cylinders have not received much attention. Intuitively, a natural convection boundary layer adjacent to a cylinder of a large radius may present similar instabilities to those on a heated flat plate. As the cylinder radius decreases, the curvature of the cylinder is expected to become increasingly important for the instabilities of the adjacent boundary layer.

The dependence of the base temperature and velocity profiles (without any perturbations) on the aspect ratio has been examined by the present authors previously [7]. It is found that in general the temperature profile bends towards the surface of the cylinder as the aspect ratio of the cylinder increases. The variation of the velocity profile due to the increase of the aspect ratio is much more complicated, which deforms towards the cylinder surface, with a decrease of the maximum velocity.

In the present study, the Ra_c dependence of boundary layers on the curvature effect of isothermally heated vertical cylinders is studied by direct stability analyses. To obtain insight into the mechanism resulting in the surface curvature effect of surface on Ra_c, the kinetic energy balance of the boundary layer is also examined.

Problem Formulation

Under consideration is the steady-state natural convection boundary layer developed adjacent to the outer surface of an isothermally heated vertical cylinder. The physical system considered in this study is schematically depicted in figure 1(*a*), in which the radius of the cylinder is R_0 and the height is H. The thermal and velocity boundary layers adjacent to the cylinder surface are characterised by the Rayleigh number Ra, the Prandtl number Pr, and the aspect ratio of the cylinder A, which are defined as follows.

$$Ra = \frac{g\beta(T_W - T_\infty)H^3}{\nu\kappa},\ Pr = \frac{\nu}{\kappa} \text{ and } A = \frac{H}{R_0} \qquad (1)$$

where g and ΔT are the gravitational acceleration (m/s^2) and the temperature difference ($T_W - T_\infty$, K) between the isothermal surface and the ambient respectively; β, ν and κ are the thermal expansion coefficient (K^{-1}), the kinematic viscosity (m^2/s^1) and the thermal diffusivity (m^2/s^1) of the working fluid at the reference (ambient) temperature.

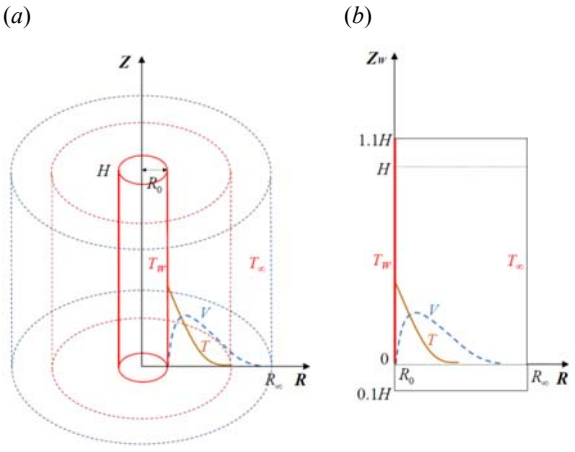

Figure 1. (*a*) Schematic of a natural convection boundary layer on a heated vertical cylinder; and (*b*) the computational domain adopted for numerical simulations.

Numerical Method

Governing Equations

The boundary layer under consideration is developing adjacent to an isothermally heated vertical cylinder of radius R_0. The computational domain adopted here is of dimensions $R_\infty\times H$, where H is the height of the vertical cylinder and R_∞ is the width in the radial direction, as sketched in figure 1(*b*). In this study, R_∞ is chosen to be about 10 times the estimated thickness of the viscous boundary layer to ensure the far-field boundary condition is satisfied. A similar treatment is adopted in [8]. Similar to the treatments used in [9], the computational domain is extended at the top and bottom by H_t=H_b=0.1H respectively to minimize the effects of the end boundaries.

The convective flow under consideration is described by the 2D Navier-Stokes and energy equations with the Boussinesq approximation. The dimensionless form of the equations in a cylindrical coordinate system is written as:

$$\frac{1}{r}\frac{\partial(ru)}{\partial r}+\frac{\partial v}{\partial z}=0 \tag{2}$$

$$\frac{\partial u}{\partial \tau}+\frac{1}{r}\frac{\partial(ruu)}{\partial r}+\frac{\partial(vu)}{\partial z}=-\frac{\partial p}{\partial r}+\frac{\Pr}{Ra^{1/2}}\left[\frac{\partial}{\partial r}\left(\frac{1}{r}\frac{\partial(ru)}{\partial r}\right)+\frac{\partial^2 u}{\partial z^2}\right] \tag{3}$$

$$\frac{\partial v}{\partial \tau}+\frac{1}{r}\frac{\partial(ruv)}{\partial r}+\frac{\partial(vv)}{\partial z}=-\frac{\partial p}{\partial z}+\frac{\Pr}{Ra^{1/2}}\left[\frac{1}{r}\frac{\partial}{\partial r}(r\frac{\partial v}{\partial r})+\frac{\partial^2 v}{\partial z^2}\right]+\Pr\theta \tag{4}$$

$$\frac{\partial \theta}{\partial \tau}+\frac{1}{r}\frac{\partial(ru\theta)}{\partial r}+\frac{\partial(v\theta)}{\partial z}=\frac{1}{Ra^{1/2}}\left[\frac{1}{r}\frac{\partial}{\partial r}(r\frac{\partial \theta}{\partial r})+\frac{\partial^2 \theta}{\partial z^2}\right] \tag{5}$$

where r, z, u, v, τ, p and θ are respectively the dimensionless forms of R, Z, U, V, t, P and T, which are made dimensionless by

$$r=\frac{R}{H},\quad z=\frac{Z}{H},\quad u=\frac{U}{V_0},\quad v=\frac{V}{V_0},\quad \tau=\frac{t}{(H/V_0)},\quad p=\frac{P}{\rho V_0^2},\quad \theta=\frac{T-T_0}{T_0-T_W} \tag{6}$$

u and v are the velocity components in the radial (r) and the vertical (z) directions; τ, p and θ are the time, pressure and temperature. $V_0=\kappa Ra^{1/2}/H$ is the characteristic velocity of a natural convection boundary layer for Pr>1.

The fluid in the computational domain is initially stationary and isothermal at a temperature θ=1. At time τ=0 the temperature of the surface at $r=r_0$ is raised to θ=1 and maintained afterwards. Open boundary conditions are applied to the top and far field boundaries. The bottom boundary of the extended computational domain is rigid, no-slip and adiabatic. Similarly, the downward extension of the cylinder surface at $r=r_0$ is assumed to be rigid, no-slip and adiabatic.

To introduction numerical perturbations into the flow, temperature perturbations are prescribed as:

$$\xi=2A_p(rand(0,1)-0.5) \tag{7}$$

where $rand(0,1)$ is a random number generator, generating statistically uniformly distributed random numbers between 0 and 1. A_p is the perturbation amplitude, which is chosen to be A_p = 5 for the present study. It is worth clarifying that the critical Rayleigh number Ra_c to be determined in this study is A_p independent.

Numerical Method

In the present study, the discretized governing equations are solved using a finite-volume based fractional pressure-velocity coupling method. The QUICK third-order upwind scheme [10] is adopted for the advection terms. The standard second-order central-differencing schemes are used for viscous, pressure gradient, and divergence terms. The second-order backward scheme is applied to time discretization. The code has been widely used and validated for buoyancy dominated boundary layer flows [8, 11-13]. The mesh (90(r) ×600(z)) is constructed with concentrated grids in the proximity of the curved surface and have a 0.3~2% linear stretching in the radial (r) direction, whereas the grids are uniform in the vertical (z) direction.

Results and Discussion

Prior to the discussion of results, it is worth clarifying that the dependence of the critical Rayleigh numbers to be determined in this study is perturbation amplitude independent. Figure 2 shows the streamwise profile of u_{RMS}/A_p obtained with three different perturbation amplitudes. It is seen in the figure that the region where amplification onsets is almost identical for the cases with A_p=5 and A_p=2.5. The critical Rayleigh number is determined to be 1.17×10^6 and the critical position is indicated by the red dotted line. The selection of A_p in this study is therefore appropriate.

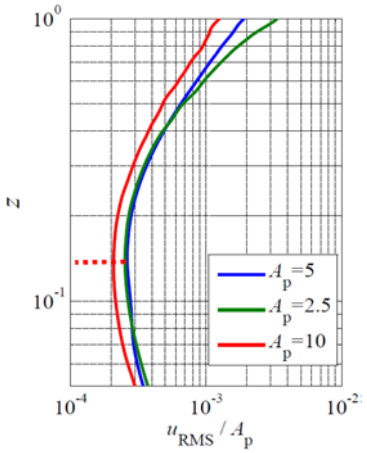

Figure 2. Dependence of critical Rayleigh number on numerical perturbation amplitude. A=0.

To obtain insight into the curvature effect on the critical Rayleigh number for the instability of the natural convection boundary layers, the streamwise profiles of the standard deviation of the streamwise velocity u_{RMS} and temperature θ_{RMS} are shown in figure 3. The velocity and temperature are obtained in the quasi-steady state of the boundary layer flow.

It is seen in figure 3 that the evolution of momentum and thermal disturbances varies significantly as the aspect ratio A increases from 0 to 2400. The streamwise profiles of u_{RMS} and temperature θ_{RMS} suggest that the amplification of the momentum and thermal disturbances reduces as the aspect ratio A increases.

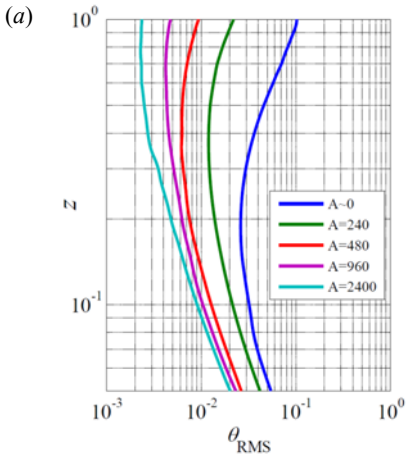

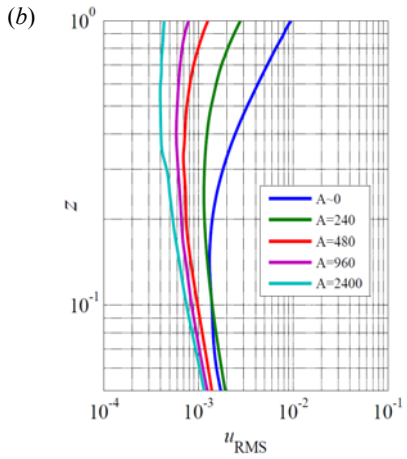

Figure 3. Streamwise profiles of root-mean-square of (*a*) streamwise velocity components and (*b*) temperature.

To determine the critical Rayleigh number Ra_c, the momentum and thermal fluctuations at streamwise neighbouring locations are compared, as indicated by the red dotted line. It is worth noting that the results for the streamwise location z<0.05 are not shown, where perturbations are dominant.

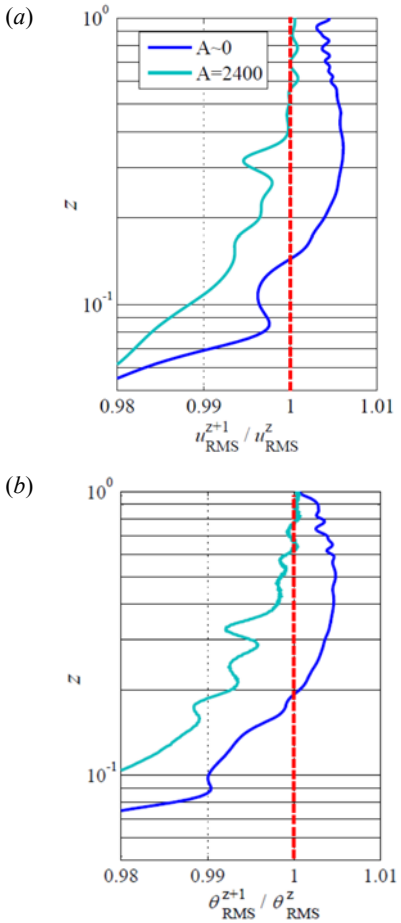

Figure 4. Streamwise amplification and decaying of (*a*) momentum and (*b*) temperature.

It is seen in figure 4 that the critical position for the flat plate (A=0) case is determined to be the location where $u^{z+1}_{RMS} / u^{z}_{RMS} > 1$ or $\theta^{z+1}_{RMS} / \theta^{z}_{RMS} > 1$, which is z=0.14 and z=0.19 from the momentum and thermal curves, as indicated by the horizontal dotted lines. An earlier beginning of momentum transition than that of the thermal transition was also observed by Jaluria *et al.*[14], which suggests that there may exist 'different' critical Rayleigh numbers Ra_c for momentum and thermal field of a boundary layer, although the difference is not remarkable. Based on the critical position z=0.14, the critical Rayleigh number Ra_c is calculated to be 1.17×10^6, which is in good agreement with the linear stability result $Ra_c=1.27\times10^6$ [1].

For the cylinder case of A=2400, the critical position is determined to be z=0.57 and z=0.53 from the momentum and thermal curves, respectively. The critical position is consistently and significantly delayed comparing to that determined in the flat plate case. Based on the critical position z=0.57, the critical Rayleigh number Ra_c is calculated to be 7.13×10^7.

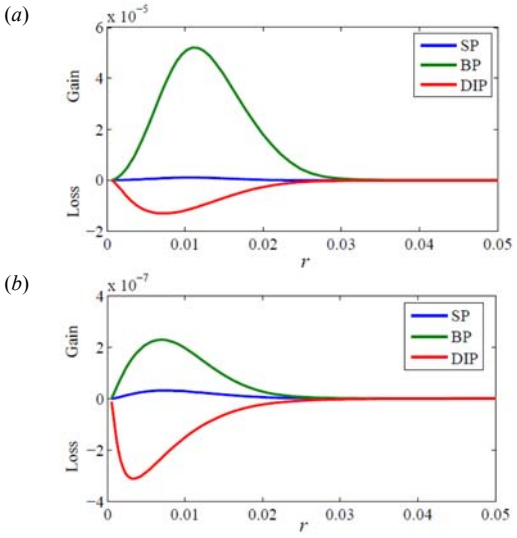

Figure 5. Kinetic energy balance (*a*) flat plate case and (*b*) cylinder case of A=2400. Results for y=0.5. SP, BP and DIP denotes shear production, buoyancy production and dissipation, respectively. The unit of SP, BP and DIP is m^2/s^3.

Figure 5 shows the kinetic energy balance for the flat plate case and the cylinder case of A=2400, respectively. The shear production (*SP*), buoyancy production (*BP*) and dissipation (*DIP*) are calculated as below:

$$SP = -\overline{U_i' U_j'} \frac{\partial \overline{U_i}}{\partial X_j}, \tag{8}$$

$$BP = g\beta \overline{U_i' T'} \delta_{i2}, \tag{9}$$

$$DIP = -\nu \overline{(\frac{\partial U_i'}{\partial X_j})^2}. \tag{10}$$

where the prime symbols denote fluctuation quantities and symbols with an overbar denote mean values. δ_{i2} is the kronecker delta. It is worth noting that the SP, BP and DIP are calculated dimensionally.

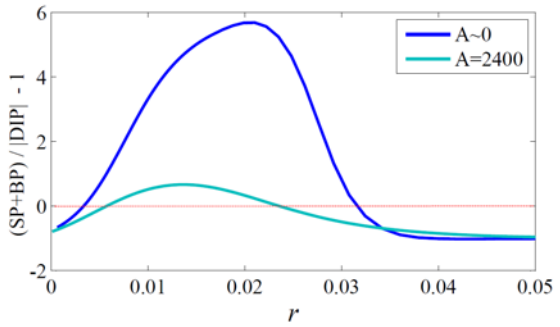

Figure 6. Ratio of production terms to the dissipation term. Positive values suggest the boundary layer being unstable. Results for z=0.5.

It is seen in figure 5 that the buoyancy production of the flat plate case is orders of magnitude larger than that of the cylinder case. To better understand the ratio of production to dissipation, the quantity $(SP+BP)/|DIP|-1$ is examined and shown in figure 6. A positive value of the quantity suggests that the boundary layer is unstable. Accordingly, it is seen in the figure that for the examined position the boundary layer of the flat plate case is much more unstable than that of the cylinder case. This characteristic also presents at other locations.

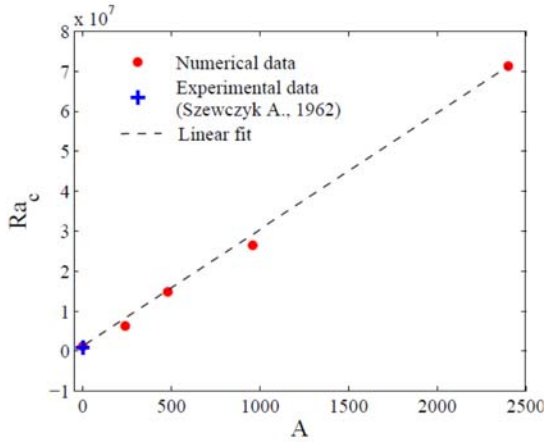

Figure 7. Dependence of the critical Rayleigh number Ra_c on the aspect ratio A of the cylinder.

The critical Rayleigh numbers Ra_c for the cylinder cases of A = 240, 480 and 960 are obtained by the method illustrated in figure 4. The dependence of the critical Rayleigh number Ra_c on the aspect ratio of the cylinder is shown in figure 7. The critical Rayleigh number of the flat plate case can be recognised as the cylinder case of an infinite radius, that is $A \sim 0$. This critical Rayleigh number is in a good agreement with the theoretical value obtained by the linear stability analysis [1].

It is seen in the figure that the critical Rayleigh number Ra_c depends linearly on the aspect ratio A linearly. As the aspect ratio A increases, that is the curvature of the cylinder becomes more significant, the critical Rayleigh number Ra_c increases and the boundary layer over the cylinder is more stable.

Conclusions

The curvature effects of isothermally heated vertical cylinders on the critical Rayleigh number Ra_c of natural convection boundary layers (Pr=7) are investigated by direct stability analyses (DSA). The aspect ratios of cylinders are A=240,480,960 and 2400. It is found that as the aspect ratio of the cylinder increases, the boundary layer over the cylinder becomes more stable, which results in a larger critical Rayleigh number. The mechanism contributing to this variation may be associated with the relatively low ratio of energy production to dissipation. A linear dependence of the critical Rayleigh number Ra_c on the aspect ratio A is also revealed.

Acknowledgments

The financial support by the Australian Research Council through Discovery Projects grant DP170104023 is gratefully acknowledged.

References

[1] Szewczyk, A.A., Stability and transition of the free-convection layer along a vertical flat plate, *International Journal of Heat and Mass Transfer*, **10**, 1962, 903-914.

[2] Armfield, S. & Janssen, R., A direct boundary-layer stability analysis of steady-state cavity convection flow, *International Journal of Heat and Fluid Flow*, **6**, 1996, 539-546.

[3] Polymeropoulos, C.E. & Gebhart, B., Incipient instability in free convection laminar boundary layers, *Journal of Fluid Mechanics*, **02**, 1967, 225-239.

[4] Armfield, S.W. & Patterson, J.C., Wave properties of natural-convection boundary layers, *Journal of Fluid Mechanics*, 1992, 195-211.

[5] Patterson, J.C., Graham, T., Schöpf, W. & Armfield, S.W., Boundary layer development on a semi-infinite suddenly heated vertical plate, *Journal of Fluid Mechanics*, 2002, 39-55.

[6] Zhao, Y., Lei, C. & Patterson, J.C., A PIV measurement of the natural transition of a natural convection boundary layer, *Experiments in Fluids*, **1**, 2015, 1-10.

[7] Zhao, Y., Lei, C. & Patterson, J.C., Effects of surface curvature on the thermal boundary layer developing along the surface of an isothermally heated vertical cylinder, *Proc. of 7th Int. Symp. on Adv. in Computational Heat Transfer. Naples, Italy.*, 2017, 1925-1933.

[8] Zhao, Y., Lei, C. & Patterson, J.C., Resonance of the thermal boundary layer adjacent to an isothermally heated vertical surface, *Journal of Fluid Mechanics*, 2013, 305-336.

[9] Lin, W., Armfield, S.W. & Patterson, J.C., Unsteady natural convection boundary-layer flow of a linearly-stratified fluid with on an evenly heated semi-infinite vertical plate, *International Journal of Heat and Mass Transfer*, **1–2**, 2008, 327-343.

[10] Leonard, B.P., A stable and accurate convective modelling procedure based on quadratic upstream interpolation, *Computer Methods in Applied Mechanics and Engineering*, **1**, 1979, 59-98.

[11] Zhao, Y., Lei, C. & Patterson, J.C., Transition of natural convection boundary layers - a revisit by Bicoherence analysis, *International Communications in Heat and Mass Transfer*, 2014, 147-155.

[12] Zhao, Y., Lei, C. & Patterson, J.C., Natural transition in natural convection boundary layers, *International Communications in Heat and Mass Transfer*, 2016, 366-375.

[13] Zhao, Y., Lei, C. & Patterson, J.C., K-type and H-type transitions of natural convection boundary layers, *Journal of Fluid Mechanics*, 2017, 352-387.

[14] Jaluria, Y. & Gebhart, B., On transition mechanisms in vertical natural convection flow, *Journal of Fluid Mechanics*, **02**, 1974, 309-337.